# Slow kinetics of iron binding to marine ligands in seawater measured by isotope exchange liquid chromatography inductively coupled plasma mass spectrometry.

Rene M. Boiteau[1*] and Daniel J. Repeta[2]

[1]College of Earth, Ocean, and Atmospheric Sciences, Oregon State University, Corvallis OR 97330, United States

[2]Department of Marine Chemistry and Geochemistry, Woods Hole Oceanographic Institution, Woods Hole, MA 02543, United States

*Corresponding Author, Rene.Boiteau@oregonstate.edu

**Abstract:**

Current understanding of dissolved iron (Fe) speciation in the ocean is based on two fundamentally different approaches; electrochemical methods that measure bulk properties of a heterogeneous ligand pool, and liquid chromatography mass spectrometry methods that characterize ligands at a molecular level. Here, we describe a method for simultaneously determining Fe ligand dissociation rate constants ($k_d$) of suites of naturally occurring ligands in seawater by monitoring the exchange of ligand-bound $^{56}Fe$ with $^{57}Fe$ using liquid chromatography-inductively coupled mass spectrometry. Values of $k_d$ were determined for solutions of ferrichrome and ferrioxamine E. In seawater, the dissociation rate constant of ferrichrome ($k_d = 10 \times 10^{-8}$ $s^{-1}$) was greater than that of ferrioxamine E ($k_d = 3.6 \times 10^{-8}$ $s^{-1}$). Rates for both compounds were over twice as fast in seawater compared with pure water, suggesting that seawater salts accelerate

dissociation. Isotope exchange experiments on organic extracts of natural seawater indicated that ligand binding sites associated with chromatographically unresolved dissolved organic matter exchanged Fe more quickly ($k_d$ = 1.8x10$^{-5}$ s$^{-1}$) than amphibactin siderophores ($k_d$ = 2.15x10$^{-6}$ s$^{-1}$) and an unidentified siderophore with *m/z* 709 ($k_d$ = 9.6x10$^{-6}$ s$^{-1}$). These findings demonstrate that our approach can bridge molecular level ligand identification with kinetic and thermodynamic metal-binding properties.

**Key words:**

Siderophore, Ocean Biogeochemistry, Metal Complexation, Reaction Rates

**Synopsis:**

We present a method for determining iron dissociation rates of chemical species in environmental mixtures containing diverse iron-complexes.

**TOC image:**

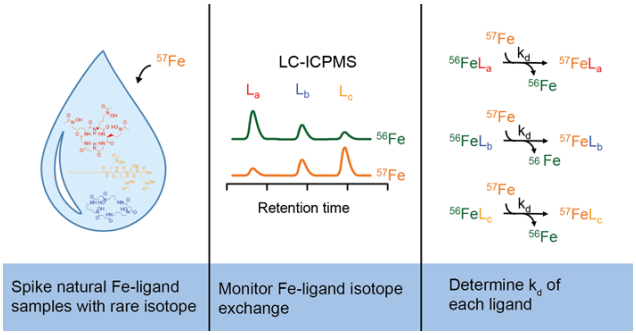

## Introduction:

Organic complexation affects the solubility, reactivity, and biological availability of many transition metals in the ocean. Since the discovery that iron (Fe) limits biological productivity in large areas of open ocean [1–4], there has been significant interest in understanding the role of organic ligands in microbial trace metal acquisition and incorporating trace metal ligand interactions into ocean biogeochemical models. Organic ligands complex over 99% of dissolved Fe in the ocean [5–9] and maintain dissolved Fe stocks available for biological uptake that are well above the solubility of inorganic Fe species in seawater [10–12]. Current methods for characterizing organic ligands focus on either measuring the Fe binding strengths of the total ligand pool, or molecular-level identification of metal-ligand complexes. Here, we bridge the gap between these approaches by developing an isotope exchange method to measure the kinetic dissociation rate, which is directly related to binding strength, of chromatographically resolved Fe-ligand complexes.

Previous research on ligand characterization has largely focused on the concentrations and binding strengths of the entire suite of ligands in a sample of seawater. These measurements have been made throughout the ocean using competitive ligand exchange (CLE) methods monitored by cathodic stripping voltammetry [13,14]. CLE experiments have demonstrated that the concentrations and binding strengths for organic Fe-binding ligands vary extensively throughout the ocean. Surface and coastal waters tend to have higher concentrations of metal binding ligands than the oligotrophic or deep ocean, suggesting that marine organic ligands have multiple important sources including

biological productivity and terrestrial inputs. Furthermore, the conditional Fe binding stability constants (log $K^{cond}_{Fe'L}$) vary spatially and a wide range of values have been reported by different studies (10.3-13.9) [13,15]. Stability constants derived from these measurements are strongly dependent on methodological setups such as added ligand identity/concentration and equilibration times [16]. Typically, one or two ligand classes with different binding strengths are fit to CLE titration data. When a two ligand fit has been used, the strong class ($L_1$) is generally more abundant in productive surface waters [6,17–20], suggesting a biological source for the strongest ligands. Weaker ligands ($L_2$) tend to be particularly abundant near continental shelves and benthic boundary layers [21–24]. Based on the similarity of binding strengths, it has been suggested that the $L_1$ class may include siderophores, biomolecules that are synthesized by microbes specifically to acquire Fe under Fe-stressed conditions [6], and that the $L_2$ class includes polysaccharides and refractory 'humic-like' organic matter produced from biomass degradation [25–29].

More recently, the molecular-level composition of Fe binding ligands has been studied with liquid chromatography with inductively coupled plasma mass spectrometry and high resolution electrospray mass spectrometry (LCMS) based approaches (Boiteau et al., 2019; Boiteau et al., 2016; Bundy et al., 2018; Gledhill et al., 2004; Macrellis et al., 2001; Mawji et al., 2008; Velasquez et al., 2011). These techniques physically separate organic ligands, identify each species based on mass spectral data and chromatographic retention time, and quantify the amount of metal associated with each. Using this approach, a broad suite of siderophores and siderophore-like compounds have been identified in seawater. In addition, nearly all seawater samples have been shown to have

a complex suite of Fe binding ligands that are chromatographically unresolved and likely generated from the degradation of biomolecules into refractory compounds with extreme structural variability.

A major challenge that remains is to link the chemical/structural information obtained by LCMS based approaches to the binding strengths acquired by CLE measurements. This requires new ways of determining physical parameters (e.g. thermodynamic and kinetic constants) of the compounds detected by LCMS that can be compared to those measured with CLE. The conditional stability constant of an organic ligand with respect to inorganic Fe is related to the formation and dissociation of that ligand with Fe. Association rates of organic ligands with free metals are generally limited by the loss of water from the inner coordination sphere of the metal species ($k_{-w}$), with only small variations attributed to the incoming ligand [37]. Dissociation rates, however, are strongly influenced by the specific structural characteristics of the ligand, and thus the disjunctive dissociation rate constant ($k_{dis}$) and ligand strength are inversely correlated. Measurements of the dissociation rate of ligand-organic complexes can therefore provide estimates of $K^{cond}_{Fe'L}$, a key parameter for incorporating Fe into ocean biogeochemical models. Previous studies have used electrochemical methods [38–41] or radioisotope exchange [42,43] to measure kinetic constants of Fe binding by marine organic ligands, but these approaches obtain average values that represent a complex ligand mixture.

Here, we introduce an approach for determining compound specific Fe dissociation rates from a mixed ligand sample based on the exchange of naturally

abundant $^{56}Fe$ with the rare $^{57}Fe$ isotope. This method provides a means of determining the dissociation rates of individual Fe ligands under close-to-natural seawater conditions and ligand concentrations. We developed this approach by measuring the dissociation rate of two model siderophores. From these rates, we used previous measurements of the conditional formation constant ($k_f$) of the model siderophores in seawater to calculate their conditional stability constants and compared these values to previous measurements obtained by electrochemistry. We then analyzed a complex mixture of naturally occurring ligands isolated from the coast of California containing chromatographically unresolved natural organic matter and two siderophore classes [35]. We compare results from isotope exchange with previous kinetic and stability constants determined by other means, and discuss the implications of our findings in the context of metal exchange across the ocean.

**Methods:**

*Iron ligand exchange kinetics:*

Measurements of dissociation rates for individual compounds in a complex mixture require a method that can determine the amount of metal associated with each species. Chromatography coupled with mass spectrometry can achieve compound specific detection, but the measurements are subject to changes in speciation during sample preparation or chromatographic separation (e.g. loss of metal from the organic ligand). To circumvent this issue, we employed isotopic exchange to determine the dissociation rates of Fe bound to siderophores and natural suites of organic ligands in seawater. For these experiments, organic ligands were first bound with natural Fe (92%

136 $^{56}$Fe). Then, a higher concentration of the rare isotope $^{57}$Fe was added as a stock solution
137 containing excess citrate as a weak stabilizing ligand to limit Fe precipitation. The
138 isotopic ratios of the organic-ligand complexes were measured over time as the two
139 isotopes equilibrated with the organic ligands. Since association rates are much faster
140 than dissociation rates for strong Fe ligands, the rate of isotopic equilibration is directly
141 related to the rate of the slow dissociation step.
142 Iron exchange can proceed via a two-step disjunctive mechanism, in which a Fe-
143 ligand complex (FeL) dissociates, followed by ligand complexation with a different Fe
144 atom, or by an adjunctive mechanism which involves the formation of a ternary complex
145 intermediate with free added citrate (Y′) or another free ligand or cation in solution. The
146 rate of isotope exchange depends on the molar fractional abundance of $^{56}$Fe ($f_{56Fe}$) in the
147 sample. The overall mole fraction of $^{56}$FeL remaining at time t can be described as a
148 pseudo-first order integrated rate equation relative to the initial concentration:
149
150 $$\left[\frac{^{56}FeL}{Ltotal}\right] = \left(\left[\frac{^{56}FeL}{Ltotal}\right]_{initial} - f_{56Fe}\right) * e^{-k_d t} + f_{56Fe} \quad (1)$$
151
152 Where $k_d$ is the pseudo first order dissociation rate constant for the metal ligand complex
153 at a particular temperature and solution composition, and includes both disjunctive ($k_{dis}$)
154 and adjunctive ($k_{adj}$) rate constants:
155
156 $$k_d = \left(k_{dis} + k_{adj,Y}[Y']\right) \quad (2)$$
157

The derivation of equation 1, provided as supporting information (SI), assumes that the concentration of added $^{57}$Fe-citrate is much larger than the initial $^{56}$Fe concentration and that the only significant forms contributing to the total ligand concentration [$L_{total}$] are the complexes with $^{56}$Fe or $^{57}$Fe. The dissociation rate constant $k_d$ can be obtained from the slope of the linear fit to the rearranged form of equation 1:

$$\ln\left(\left[\frac{^{56}FeL}{Ltotal}\right] - f_{56Fe}\right) = -k_d t + \ln\left(\left[\frac{^{56}FeL}{Ltotal}\right]_{initial} - f_{56Fe}\right) \quad (3)$$

A key aspect of this method is that liquid chromatography with inductively coupled plasma mass spectrometry (LC-ICPMS) is capable of simultaneously measuring isotope ratios (and thus $k_d$) for every chromatographically resolved metal species in a sample. The determination of the isotopic ratio, such as $^{56}$FeL/($^{56}$FeL + $^{57}$FeL), by LC-ICPMS is a robust measurement that is not impacted by Fe loss during extraction or chromatography, and does not vary with changes in instrument sensitivity. Although isotopic fractionation effects do affect isotopic ratios, these fractionation factors are very small (typically <<1%) compared to the changes that are measured in this study [44–46]. As illustrated by equation 2, the excess free citrate that was amended to samples can accelerate the rates of Fe-ligand exchange via adjunctive pathways compared to unamended samples. As a result, measurements of $k_d$ described here can be viewed as upper bounds on the disjunctive dissociation rate constants ($k_{dis}$) of ligands in natural waters.

*Materials and reagents:*

High purity water (18.2 MΩ $cm^{-1}$, $qH_2O$) and LCMS grade methanol (MeOH) and ammonium formate (Optima, Fisher scientific) were used in this study. The methanol was redistilled in a polytetrafluoroethylene (PTFE) still to reduce the Fe blank. Polycarbonate carboys and PTFE tubing for sample collection and solid phase extraction (SPE) were soaked overnight in 0.1% detergent (Citranox), rinsed with $qH_2O$, and soaked for 1 day in 1 M HCl (trace metal grade, Fisher Scientific) before a final $qH_2O$ rinse. Stock solutions of ferrichrome, ferrioxamine E and cyanocobalamin (Sigma Aldrich) were prepared in $qH_2O$. To prepare the $^{57}Fe$ citrate stock solution, $^{57}Fe$ oxide (96% $^{57}Fe$, Cambridge Isotope Laboratories) dissolved in concentrated HCl (trace metal grade), and diluted to 4 µM Fe in a 5 mM citrate solution prepared from trisodium citrate dihydrate (Fisher scientific) in $qH_2O$. The 1000-fold excess of citrate was added to prevent the precipitation of ferric Fe oxyhydroxides. Citrate was selected due to its fast dissociation kinetics [47,48], which exchanges Fe isotopes rapidly while maintaining a high concentration of dissolved Fe.

*Sample collection:*

The sample used for the natural ligands Fe exchange rate experiment was obtained from surface waters (3m depth) within a cyclonic (upwelling) eddy along the coast of California in July 2014 IRNBRU cruise from 39.43°N, 124.54°W. A volume of 20 L was collected using a trace metal clean GeoFish sampling system and passed through a 0.2 µm polyethersulfone capsule filter into a 20 L polycarbonate carboy. The dissolved Fe concentration was measured at 0.12 nM by flow injection analysis, while total solid phase extractable Fe ligand concentrations and siderophore concentrations

were measured by LC-ICPMS to be 0.17 nM and 5 pM respectively [35]. Organic compounds were extracted from the seawater onto a solid phase extraction (SPE) resin column (1 g, ENV, Agilent) at a flow rate of 15 mL/min using a peristaltic pump equipped with polytetraflouroethylene (PTFE) and platinum-cured silicone tubing. Prior to use, the SPE column was activated with 5 mL MeOH, rinsed with 10 mL pH 2 $qH_2O$ (acidified with trace metal grade HCl), and conditioned with 10 mL $qH_2O$. The column was rinsed with 10 mL of $qH_2O$ after extraction to remove excess salt and immediately frozen. To recover natural organic ligands, the column was thawed, eluted with 6 mL MeOH, and the MeOH extract was amended with 10 µL of a 50 µM cyanocobalamin stock solution as an internal standard. The extract was concentrated to <1 mL under a stream of $N_2$ gas and brought up to a volume of 2 mL with $qH_2O$.

*Fe exchange from ferrichrome and ferrioxamine E in seawater:*

Two solutions containing 2 nM each of ferrioxamine E, ferrichrome, and cyanocobalamin were prepared in 60 mL PTFE bottles, one containing 50 mL $qH_2O$ and another containing 50mL filtered seawater. To each bottle, 1 mL of the $^{57}Fe$ citrate stock solution was added, yielding a final concentration of 98 µM citrate and 78 nM added $^{57}Fe$ and a pH of 5.8. The solutions were filter sterilized through 0.2 µm polyethersulfone syringe filters (Millipore) into microwave sterilized polycarbonate bottles. The $f_{56Fe}$ of the solutions was measured by ICPMS to be 0.11 ± 0.005. The bottles were incubated in the dark to prevent photodegradation at room temperature with time points collected over the course of 235 days by passing 4 mL from each treatment through a 100 mg C18 SPE column (Bond Elut, Agilent) that had been activated with MeOH and rinsed with $qH_2O$.

227 The columns were then rinsed with 1 mL $qH_2O$ to remove salts and excess $^{57}Fe$ citrate,
228 which is not retained by the column. The columns were stored at -20 °C. For analysis,
229 siderophores were eluted with 0.8 mL of MeOH, the solvent was removed by vacuum
230 centrifugation (Savant speedvac), and samples diluted to a final volume of 150 µL with
231 $qH_2O$. Samples were analyzed within hours to minimize Fe exchange during processing.
232
233 LC-ICPMS analysis was used to quantify isotope ratios for separated ligands
234 using methods adapted from previous studies [34,35,49]. Organic extracts were separated on a
235 bioinert high pressure liquid chromatography (HPLC) system (Dionex Ultimate RSLC
236 3000) fitted with a C18 column (Hamilton, 2.1x150 mm, 3 µm particle size) and
237 polyetheretherketone (PEEK) tubing and connectors. Samples were eluted with (A) 5
238 mM aqueous ammonium formate and (B) 5 mM ammonium formate in distilled MeOH
239 using a 12 minute gradient from 10-60% B, followed by isocratic elution at 60% B for 5
240 minutes at a flow rate of 0.2 mL/min. 50 µL/min of the eluent flow was directed to a
241 quadrupole ICPMS (Thermo iCAPq) by a post column PEEK tee. $O_2$ gas (25 mL/min)
242 was added to the plasma to completely oxidize the organic solvent to $CO_2$. Data was
243 collected in kinetic energy discrimination mode monitoring $^{56}Fe$, $^{57}Fe$, and $^{59}Co$ with a
244 dwell time of 0.1 seconds using 4.5 mL/min He as a collision gas to remove the $ArO^+$
245 interference on $^{56}Fe$. Isotopologues were quantified based on the integration of
246 chromatographic peak areas above the baseline, with sub picomole detection limits. The
247 mean and standard deviation of isotope ratios measured by LC-ICPMS was evaluated by
248 repeated analyses of siderophores bound to naturally occurring Fe. The $^{57}Fe/^{56}Fe$
249 measurement was 0.026±0.001 (n=6), which is slightly higher than the natural abundance

ratio of 0.023. This reflects typical instrumental mass bias towards heavier isotopes[50] and indicates high precision in the context of the isotope ratios measured this study. A linear regression was fit to a plot of $\ln[^{56}Fe/(^{56}Fe+^{57}Fe) - f_{56Fe}]$ versus time for each compound and treatment. Values of $k_d$ presented in Table 1 were calculated from the slope and standard error of the fit.

*Fe exchange of natural organic ligands:*

To investigate Fe exchange by natural organic ligands from seawater, 40µL of the $^{57}$Fe citrate stock solution was mixed with 160 µL of the concentrated organic extract from the California coast in a 250 µL autosampler vial insert (Agilent Scientific). Note that these extracts were preconcentrated by a factor of 10,000 via solid phase extraction, so the sample contains lower salt content and higher organic matter/ligand concentrations. The resulting spiked solution contained 1 mM citrate, 800 nM added $^{57}$Fe and $f_{56Fe} = 0.21 \pm 0.01$ and a pH of 8.1. This sample was analyzed by LC-ICPMS after incubating at 25 °C for 30 minutes, 4 days, and 10 days using a bioinert liquid chromatography system (Agilent 1260 Series) and a quadrupole ICPMS as described above, but using a 20 minute gradient from 5-95% B, followed by a 10 minute isocratic elution at 95% B. Data was collected in kinetic energy discrimination mode monitoring $^{56}$Fe, $^{57}$Fe and $^{59}$Co with dwell times of 0.05 seconds.

**Results and discussion:**

*Fe exchange for model siderophores in seawater:*

272 We first investigated the exchange kinetics of two model siderophores,
273 ferrichrome and ferrioxamine E, in seawater (pH 8.1) and $qH_2O$ (pH 5.8). These two tri-
274 hydroxamate siderophores are produced by fungi and bacteria respectively, and
275 ferrioxamine E has been previously detected in the surface ocean [31,34–36]. The Fe
276 dissociation kinetics of ferrichrome, ferrioxamine B, and natural marine organic ligand
277 pools have been studied previously in seawater using electrochemical and radioisotope
278 exchange measurements, providing a benchmark to compare with the results from our
279 method [39,41–43,51,52].
280
281 LC-ICPMS analysis of the samples yielded chromatograms with the two
282 siderophores fully resolved (Fig. 1), and an increase in the peak intensity of $^{57}Fe$ versus
283 $^{56}Fe$ over time. Several precautions were taken to ensure that sample preparation and
284 chromatographic separation did not influence isotope ratios. Distilled solvents and trace
285 metal free extraction and chromatography components were used for this analysis to
286 prevent the siderophores of interest from exchanging with ambient Fe during sample
287 processing, which would bias the measured Fe isotope ratios. Iron may still dissociate
288 from the ligands during sample preparation or chromatography, but this has negligible
289 impacts on isotope ratios. Sterilization of the solution was found to be important to
290 prevent microbial degradation of the siderophores over time. The sum of the $^{56}Fe$ and
291 $^{57}Fe$ peak areas and thus total siderophore concentration was consistent between
292 timepoints (Fig. 1; standard deviation of 7% for ferrichrome and 6% for ferrioxamine E).
293 While the citrate concentrations used in this study have been shown to stabilize Fe over a
294 wide range of pH and ionic strength [48,53], we note that $Mg^{2+}$ and $Ca^{2+}$ also bind with

295 citrate and reduce its effectiveness at stabilizing dissolved Fe. Estimates of Fe speciation
296 in seawater (salinity of 35 and pH of 8.1) with 98 μM citrate and 78 nM Fe were
297 calculated based on the $cit^{4-}$ model Ito *et. al.* [48,53] with ionic strength corrected stability
298 constants for $Mg^{2+}$ and $Ca^{2+}$ binding with citrate.[54] These calculations suggest that only
299 67% of Fe was bound to citrate (primarily as $Fe(Cit)_2^{5-}$) and that some Fe precipitation
300 may have occurred in the seawater condition. However, this should not greatly affect the
301 rate of isotopic exchange and thus the measured dissociation constants.
302
303 Integrated peak areas were determined to calculate the $^{56}Fe/(^{56}Fe+^{57}Fe)$ ratios at
304 every time point and obtain linear fits to equation 3 for each compound (Fig. 2). Using
305 this method, dissociation rate constants for ferrichrome and ferrioxamine E were
306 determined in both $qH_2O$ and seawater (Table 1). The $k_d$ value for ferrichrome was
307 4.5±0.7 x $10^{-8}$ $s^{-1}$ in $qH_2O$ and 10±0.3 x $10^{-8}$ $s^{-1}$ in seawater, while $k_d$ for ferrioxamine E
308 was 1.7±0.1 x $10^{-8}$ $s^{-1}$ and 3.6±0.02 x $10^{-8}$ $s^{-1}$ in seawater. Our observation that
309 ferrichrome dissociation was nearly 3x faster than ferrioxamine E dissociation in both
310 $qH_2O$ and seawater is consistent with the higher reported affinity of ferrioxamine E (log β
311 = 32.49) compared to ferrichrome (log β = 29.07) for Fe [55,56].
312
313 The ferrichrome $k_d$ value for seawater is in good agreement with the value of 5±4
314 x $10^{-8}$ $s^{-1}$ obtained by *Witter et al*., 2000, who used electrochemical methods to monitor
315 the exchange of Fe bound to siderophores in UV oxidized seawater with added 1-nitroso-
316 2-naphthol (1N2N). However, the reported $k_d$ value of ferrioxamine B (150±180 x $10^{-8}$ $s^{-1}$) based on 1N2N electrochemical measurements was significantly faster than both

ferrichrome and ferrioxamine E, although the reported ferrioxamine B binding strength (log β = 30.6) is intermediate between ferrioxamine E and ferrichrome [56]. Dissociation rates measured by the 1N2N electrochemical method have also conflicted with other kinetic studies for protoporphyrin IX and phytic acid [57,58]. These discrepancies highlight the advantage of having a distinct method to measure binding constants, such as the LC-ICPMS approach described here.

For both compounds, faster dissociation kinetics were observed in seawater at pH 8.1 and 35 PSU salinity compared with $qH_2O$ at pH 5.8. The two factors that differentiate these treatments, pH and salinity, likely have opposite effects on Fe dissociation kinetics. Previous studies have shown that lower pH accelerates metal dissociation from hydroxamate siderophores [59,60] via a mechanism involving protonation of the siderophore complex, followed by adjunctive or disjunctive dissociation. Lower pH also affects the protonation state of free citrate, from predominately $HCit^{3-}$ at pH 8.1 to $H_2Cit^{2-}$ at pH 5.8, which may influence adjunctive dissociation rates involving ternary complexes. In seawater, higher concentrations of $Na^+$, $Ca^{2+}$, $Mg^{2+}$, and other cations can promote the formation of coordination complexes that weaken the Fe-siderophore association and enable faster dissociation kinetics, similar to the role of $H^+$ at lower pH. As a secondary effect, cations bind with non-metalated (free) citrate, which slows dissociation via adjunctive pathways (98% of citrate was likely present as complexes with Ca, Mg, and Na in seawater) [47,61]. The overall faster dissociation rates observed in seawater compared to $qH_2O$ suggest that the accelerating effect of seawater cations is strong.

341 The results for ferrioxamine E and ferrichrome demonstrate that monitoring $^{57}Fe$
342 exchange by LC-ICPMS is a useful approach for determining metal dissociation
343 constants. One of the primary advantages of this method is that it provides a compound
344 specific dissociation rate constant for each component within a complex mixture of
345 ligands as found in natural seawater, whereas competitive ligand exchange measurements
346 reflect the combined dissociation kinetics of all ligands simultaneously. Furthermore, less
347 than 1 picomole of compound is needed for each analysis, enabling sensitive analyses of
348 dilute solutions. The concentration of metals and ligands in solution influences the
349 contribution of adjunctive versus disjunctive mechanisms to overall reaction rates. These
350 isotope-exchange analysis can be scaled to liter volumes for natural samples containing
351 picomolar concentrations of organic ligands. Ultimately, the determination of
352 environmentally relevant rates of Fe dissociation can inform biogeochemical models of
353 Fe cycling [43].
354
355 The LC-ICPMS approach is suitable for monitoring metal ligand complexes with
356 slow exchange rates, such as siderophores, provided the complexes remain stable over
357 timescales greater than the analysis time for each measurement
358 (extraction/preconcentration time plus analysis time). It is important to consider that once
359 concentrated, ligands are capable of exchanging metal with each other, which drives their
360 isotopic composition (and thus the calculated dissociation rates) closer together if
361 exchange is fast relative to the timescale of analysis. Previous studies found that the
362 exchange of Fe between concentrated (4 mM) siderophores ferrioxamine B and
363 ferrichrome is only 50% complete after 220 hours of incubation at 25°C and pH 7.4 [60].

Thus, Fe isotope exchange between siderophores is likely negligible in the siderophore extracts before and during analysis by LC-ICPMS.

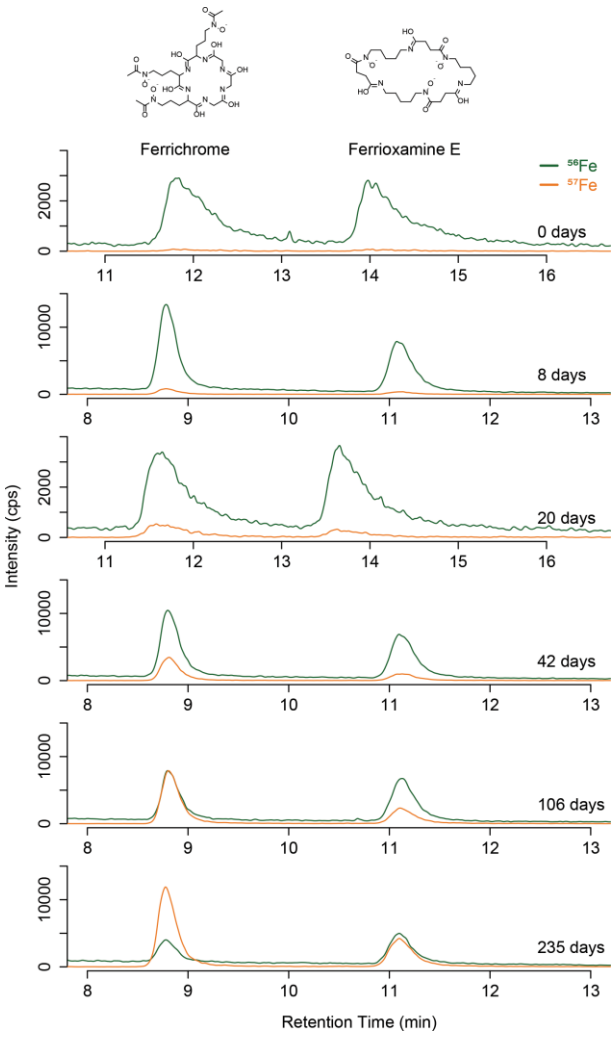


**Figure 1:** LC-ICPMS separation and detection of ferrichrome (first peak) and ferrioxamine E (later peak) extracted from seawater incubations with excess $^{57}Fe$ added. Over time, $^{56}Fe$ (green trace) is lost from the compounds and replaced with $^{57}Fe$ (orange trace). Samples from 0 and 20 days were analyzed using a different LC column than the other four samples, hence the differences in peak shape, sensitivity, and retention time compared to the other four samples.

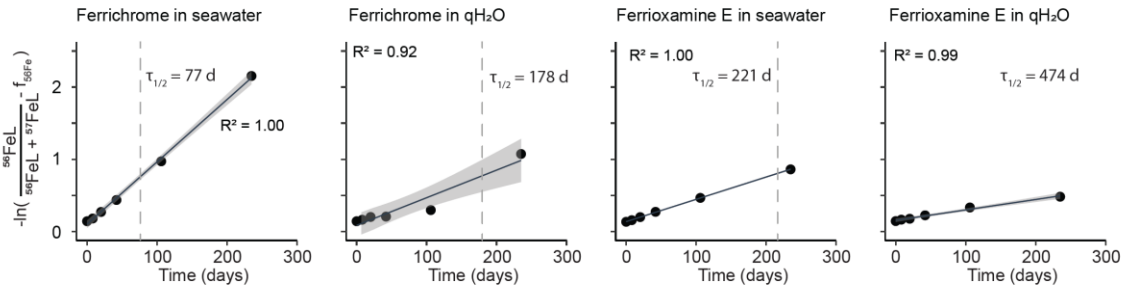


**Figure 2:** Determination of dissociation rate constant ($k_d$) for ferrichrome and ferrioxamine E in seawater and ultrapure water ($qH_2O$). Iron isotope ratios ($^{56}Fe/^{56}Fe+^{57}Fe$) of ferrichrome and ferrioxamine E were measured over time measured by LC-ICPMS during an incubation with $^{57}Fe$ citrate in seawater and $qH_2O$. Gray lines show the linear fits to the data in the form of equation 3, with a slope equal to $k_d$. Dashed lines indicate the half-life ($\tau_{1/2}$) of the Fe-complex with respect to dissociation. Gray shaded area indicates the standard error of the fit.

**Table 1: Kinetic rate constants of siderophores measured by LC-ICPMS**

| Conditions | Siderophore | $k_d$ ($s^{-1}$) x $10^{-8}$ | std error ($s^{-1}$) x $10^{-8}$ | Published $k_d$ ($s^{-1}$) x $10^{-8}$ | $\tau_{1/2}$ (d) |
|---|---|---|---|---|---|
| Seawater pH=8.1 S=35 ppt | Ferrichrome | 10 | 0.25 | 5±4* | 77 |
| | Ferrioxamine E | 3.6 | 0.022 | | 220 |
| | Ferrioxamine B | | | 150±180* | |
| | Marine NOM | | | 10-9720* | |
| | | | | 10-100 (strong)** | |
| | | | | 6000-25000 (weak)** | |
| | | | | 520-7900~ | |
| $qH_2O$ pH = 5.8 | Ferrichrome | 4.5 | 0.69 | | 178 |
| | Ferrioxamine E | 1.7 | 0.092 | | 474 |
| SPE extract pH ~ 6-8 | Amphibactins | 215 | 18 | | 3.7 |
| | Unidentified (709 m/z) | 960 | 73 | | 0.83 |
| | Unresolved DOM | 1800 | 710 | | 0.44 |

* Measured by CLE with added 1-nitroso-2-naphthol (1N2N), Luther and Wu (1997) Witter and Luther (1998), Witter et al. (2000).
** Measured by CLE with 2-(2-thiazolylazo)-4-methylphenol (TAC), Croot and Heller (2012).
~ Measured by $^{55}Fe$ radioisotope exchange, Croot and Heller (2012)

*Kinetic and stability constants of marine siderophores:*

Microbial Fe acquisition by siderophores involves secretion of the free form of the siderophore, chelation of Fe, and uptake of the Fe-siderophore complex before dissociation or decomposition. The results from LC-ICPMS analyses provide insight into the rates of these processes. Solving equation 1 for the half-maximum concentration yields half-life ($\tau_{1/2}$) timescales with respect to dissociation for ferrichrome (77d) and

404 ferrioxamine E (220d). These timescales are similar to the residence time of Fe in the
405 surface ocean [62,63]. Thus, once Fe-siderophore complexes form in the ocean, dissociation
406 is likely negligible in the absence of degradation or redox processes.
407
408 The formation and dissociation rate constants can be used to estimate equilibrium
409 conditional stability constants of the metal-ligand complex ($K^{cond}_{Fe'L}$) to compare with
410 values determined by electrochemical competitive ligand exchange methods. $K^{cond}_{Fe'L}$ is
411 related to the forward and reverse rate constants of the reaction:
412
413 $$K^{cond}_{Fe'L} = k_f/k_{dis} \quad (4)$$
414
415 The conditional formation constant ($k_f$) of the siderophore ferrioxamine B in seawater at
416 pH 8 has been previously measured by Hudson *et al.* to be 2.0 x $10^6$ $M^{-1}s^{-1}$ [37]. Since the
417 rate-limiting step of forming a strong Fe-ligand complex is the removal of inner sphere
418 water, $k_f$ constants vary little for different siderophores [64]. Although the measured $k_d$
419 value here includes a contribution from the purely disjunctive mechanism as well as
420 adjunctive mechanisms involving added free citrate, we can use it as an upper bound
421 estimate of $k_{dis}$. Using the experimentally determined $k_d$ of ferrioxamine-E in seawater
422 (3.6 x $10^{-8}$ $s^{-1}$) and the value of $k_f$ from Hudson and Morel, we calculate log $K^{cond}_{Fe'L}$ =
423 13.7. While the $K^{cond}_{Fe'L}$ determined here represents a lower bound estimate, it illustrates
424 an approach for estimating species-specific conditional stability constants. This value is
425 within a factor of two of the CLE measured stability constant for ferrioxamine E of 14.0,

426 which may also be viewed as a lower-bound estimate since the Fe-saturated ligand was
427 used [36].
428
429 *Fe isotope exchange in organic ligands of marine origin:*
430 In a previous study, we found surface waters of the upwelling transition zone in
431 the California current system contained a mixture of unresolved dissolved organic matter
432 (DOM), known siderophores (amphibactins), and an unidentified Fe ligand complex
433 (likely a hydroxamate siderophore) with a monoisotopic ion mass of 709 *m/z* and
434 molecular formula of $[C_{33}H_{59}O_8N_5Fe]^+$ [35]. We used $^{57}Fe$ exchange to investigate the
435 relative binding strengths of these compounds and the timescales required to incorporate
436 an isotopic label. A large excess of $^{57}Fe$ citrate was added to the concentrated organic
437 extract and was allowed to exchange with the natural seawater ligands for 30 minutes, 4
438 days, and 10 days before analysis by LC-ICPMS (Fig. 3). $^{56}Fe/Fe_{total}$ ratios were
439 determined by integrating the area of the $^{57}Fe$ and $^{56}Fe$ LC-ICPMS chromatograms for
440 unresolved DOM eluting between 7 to 21 min, amphibactins eluting between 25-28 min,
441 and the unidentified siderophore (709 *m/z*) eluting between 28-28.8 min (Fig. 4). An 18%
442 decrease in total dissolved Fe was observed over the course of the experiment, suggesting
443 a small amount of loss of citrate-bound Fe over time due to precipitation or adsorption
444 onto the vial walls.
445
446 Dissociation rates were measured for the three components by calculating isotope
447 ratios over time and determining the slope of the fit to equation 3. The siderophores
448 showed a gradual exchange of $^{56}Fe$ for $^{57}Fe$ over time, with measured $\tau_{1/2}$ of 0.8 days for

449 the unidentified siderophore with m/z 709 and 3.7 days for amphibactins. The unresolved
450 DOM exchanged Fe significantly faster than the siderophores. Under the experimental
451 conditions, the measured $\tau_{1/2}$ of the unresolved DOM-Fe complex with respect to
452 dissociation was 0.4 days. However, unlike the siderophores, the total Fe associated with
453 the unresolved DOM increased over time by 80%, indicating that the $^{57}Fe$ signal reflects
454 not only Fe isotope exchange, but also $^{57}Fe$ binding to excess Fe-free ligand. We also
455 investigated whether $^{57}Fe$ displaced other metals (Cu, Ni, or Zn) associated with the
456 unresolved DOM, but the LC-ICPMS chromatograms of these metals remained constant
457 over the course of the experiment. This overall increase in $^{57}FeL$ resulted in lower
458 measurements of $^{56}Fe/Fe_{total}$ associated with the unresolved DOM, and thus the true $\tau_{1/2}$
459 for the unresolved DOM was likely longer than the value calculated here. This issue
460 could be avoided in future experiments by pre-saturating ligands with $^{56}Fe$.
461
462 The Fe exchange rates determined for the natural suite of organic ligands in
463 seawater extracts are likely faster than exchange rates *in-situ* due to the added citrate and
464 10,000 fold higher concentration of natural Fe ligands in our experimental sample.
465 Higher ligand concentrations will accelerate the rates of Fe exchange by adjunctive
466 mechanisms. Although the pH of the $^{57}Fe$ amended extracts was not measured due to the
467 small volume, it was estimated to be between 6-8 due to the removal of carbonate from
468 the seawater by SPE. Lower salt concentration and lower pH in the extracts may also
469 influence Fe dissociation rate relative to seawater conditions, but our similar results
470 comparing Fe-siderophore exchange in $qH_2O$ and seawater suggest that the net effect
471 may be small.

To constrain these experimental effects, we compared the measured dissociation rates of amphibactins (2.15 x $10^{-6}$ $s^{-1}$) with estimates derived from electrochemical measurement. Given literature values of log $K^{cond}_{Fe'L}$ for amphibactins (12.06 to 12.48)[36] and assuming that the $k_f$ value for these strong hydroxamate siderophores are similar to ferrioxamine B (2.0 x $10^6$ $M^{-1}s^{-1}$), one can estimate $k_d$ = 0.7-1.7 x $10^{-6}$ $s^{-1}$. Based on this comparison, we estimate that dissociation was up to 3 times faster in the SPE organic extract compared to seawater, likely due to the contribution of adjunctive exchange mechanisms in the concentrate with added citrate. Our dissociation rate measurements also indicate that the unidentified siderophore with 709 *m/z* ($k_d$ = 9.6 x $10^{-6}$ $s^{-1}$) is a weaker Fe chelator than amphibactins.

The measured $k_d$ value for the unresolved DOM (1.8±0.7 x $10^{-5}$ $s^{-1}$) is notably faster than for the siderophores (Table 1). The dissociation rate is within the range measured for weak seawater ligands by previous studies using CLE ($k_d$ = 1 x $10^{-7}$ to 9.72 x $10^{-5}$ $s^{-1}$) and radioisotope exchange methods ($k_d$ = 5.2 x $10^{-6}$ to 7.92 x $10^{-5}$) [39,41–43,52]. As with our experiments, dissociation rates determined by CLE based methods may also be accelerated by adjunctive reactions with the added ligand. These similarities suggest that the chromatographically unresolved DOM represent a fraction of the weaker ligands in seawater detected by electrochemical methods. These ligands are likely composed of heterogeneous biomass decomposition products with a range of Fe binding strengths. Some of these ligands, which bind to Fe when it is added at high concentrations as Fe-citrate, may be too weak to keep Fe in solution in seawater over long periods of time [43]. However, they may still be important for transiently solubilizing Fe in the ocean from

benthic boundaries or atmospheric deposition. It is also likely that a small proportion of the DOM binding sites are strong enough to be indistinguishable from siderophores in terms of conditional strength. We have previously suggested that these unresolved DOM components detected by LC-ICPMS correspond, at least in part, to electrochemically active ligands detected by catalytic CSV that have a similar redox potential to humic acids [22,25,35,65]. They have similar oceanographic distributions, with elevated concentrations near the coastal margin and benthic boundary, where they may promote the transport of dissolved Fe from sediments to overlying surface waters.

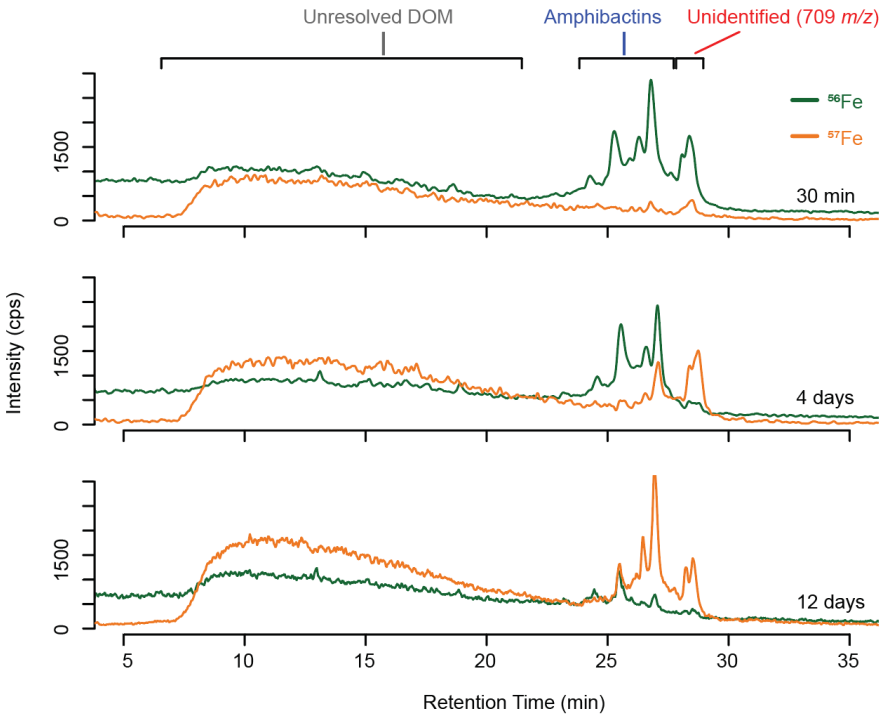


**Figure 3:** Iron isotope exchange between natural Fe ligands extracted from seawater and $^{57}$Fe-citrate by LC-ICPMS. Over time, $^{56}$Fe (green trace) dissociates from the natural ligands and is replaced with $^{57}$Fe (orange trace).

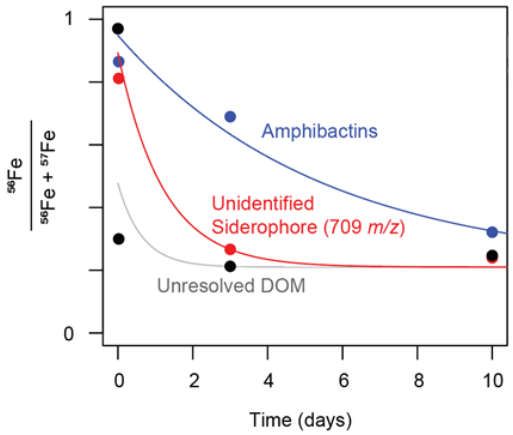


509

510 **Figure 4:** $^{56}$Fe fraction associated with each component of the natural ligand sample over
511 time. Colored lines indicate the modelled rate of Fe isotope exchange for each of the
512 three ligands (equation 1) based on the measured dissociation rate constants ($k_d$).

513

514 *Towards measurements of ligand-specific Fe dissociation rates in natural seawater:*

515 Laboratory experiments with simple model compounds have been instrumental to
516 the development of mechanistic models of aqueous metal-ligand speciation [47,48,64,66], but
517 applying such models to natural waters relies on knowledge of the composition and
518 properties of naturally occurring ligands. With the advent of LCMS methods that enable a
519 chemical characterization and quantification of organic ligands in natural seawater
520 extracts, there is an opportunity to generate more complete models of metal speciation in
521 marine waters. The experiments presented here provide a proof-of-concept that isotopic
522 exchange monitored by LC-ICPMS is a promising approach to simultaneously observe
523 the rates of Fe-ligand exchange for mixtures of organic ligands in natural seawater and to
524 estimate conditional stability constants of each component that can be
525 chromatographically separated.

526

While our results provide a starting point, further work is needed to determine the contribution of adjunctive vs. disjunctive pathways to the rate of Fe exchange in seawater, in particular those involving ternary complexes with added citrate. This can be accomplished with experiments that vary the concentration of citrate. Given the high sensitivity of the LC-ICPMS method, future experiments can measure the dissociation rates of naturally occurring ligands under ambient seawater conditions by directly amending seawater with $^{57}$Fe citrate and performing solid phase extractions and LC-ICPMS analysis of subsamples at each kinetic timepoint. Higher temporal resolution within the first few hours will also provide better constraints on the exchange kinetics of the unresolved DOM. In addition, optimizing the separation between ligand pools will enable more robust quantitation of each rate.

This work also highlights that Fe exchange kinetics in seawater are sluggish due to dissociation rates and the dilute nature of Fe and ligands. Since Fe′ is often more reactive with respect to scavenging and biological uptake than ligand bound Fe, models of Fe biogeochemistry often rely on explicit estimates of [Fe′] supplied from dissociating FeL complexes. For hydroxamate siderophores, dissociation of ferric complexes occurred on timescales that may exceed turnover times of Fe and ligands in the surface open ocean. Such slow rates highlight the importance of biological or photochemical processes for accelerate the rate of [Fe′] release from strong ligands, as has been pointed out previously by Croot et al. 2012 [43]. Further work is needed to evaluate the rate at which Fe is released from siderophores via other reactions that weaken the complex strength (e.g. siderophore degradation or Fe reduction by sunlight or reactive oxygen species).

**Supporting Information:** Derivation of kinetic equations of isotope exchange.

**Acknowledgements:**

We would like to thank Serena Dao and Geoffrey Smith for assistance collecting samples, Francois Morel for valuable discussion, and Ken Bruland and the scientists and crew of the R/V *Melville*. This work was funded by the Gordon and Betty Moore Foundation (Grant GBMF3298), the National Science Foundation (NSF) program in chemical oceanography (OCE-1356747, OCE-1259776, OCE- 1736280, OCE-1829761), the NSF Science and Technology Center for Microbial Oceanography Research and Education (DBI-0424599), and the Simons Foundation (Awards 621513, 329108).

**References:**

(1) Martin, J. H.; Gordon, R. M.; Fitzwater, S. E. The Case for Iron. *Limnol. Oceanogr.* **1991**, *36* (8), 1793–1802.

(2) Martin, J. H.; Coale, K. H.; Johnson, K. S.; Fitzwater, S. E.; Gordon, R. M.; Tanner, S. J.; Hunter, C. N.; Elrod, V. A.; Nowicki, J. L.; Coley, T. L.; Barber, R. T.; Lindley, S.; Watson, A. J.; Van Scoy, K.; Law, C. S.; Liddicoat, M. I.; Ling, R.; Stanton, T.; Stockel, J.; Collins, C.; Anderson, A.; Bidigare, R.; Ondrusek, M.; Latasa, M.; Millero, F. J.; Lee, K.; Yao, W.; Zhang, J. Z.; Friederich, G.; Sakamoto, C.; Chavez, F; Buck, K.; Kolber, Z.; Greene, R.; Falkowski, P.; Chisholm, S. W.; Hoge, F.; Swift, R.; Yungel, J.; Turner, S.; Nightingale, P.; Hatton, A.; Liss, P.; Tindale, N. W. Testing the Iron Hypothesis in Ecosystems of

the Equatorial Pacific Ocean. *Nature* **1994**, *371* (6493), 123–129. https://doi.org/10.1038/371123a0.

(3) Boyd, P. W.; Jickells, T.; Law, C. S.; Blain, S.; Boyle, E. A.; Buesseler, K. O.; Coale, K. H.; Cullen, J. J.; Baar, H. J. W. De; Follows, M.; Harvey, M.; Lancelot, C.; Levasseur, M. Mesoscale Iron Enrichment Experiments 1993–2005: Synthesis and Future Directions. *Science (80-. ).* **2007**, *315* (February), 612–617.

(4) De Baar, H.; Boyd, P.; Coale, K.; Landry, M. Synthesis of Iron Fertilization Experiments: From the Iron Age in the Age of Enlightenment. *J. Geophys. Res* **2005**, *110* (C9), 1–24. https://doi.org/10.1029/2004JC002601.

(5) Rue, E.; Bruland, K. Complexation of Iron(III) by Natural Organic Ligands in the Central North Pacific as Determined by a New Competitive Ligand Equilibration/Adsorptive Cathodic Stripping Voltammetric Method. *Mar. Chem.* **1995**, *50* (1–4), 117–138. https://doi.org/10.1016/0304-4203(95)00031-L.

(6) Rue, E. L.; Bruland, K. W. The Role of Organic Complexation on Ambient Iron Chemistry in the Equatorial Pacific Ocean and the Response of a Mesoscale Iron Addition Experiment. *Limnol. Oceanogr.* **1997**, *42* (5), 901–910. https://doi.org/10.4319/lo.1997.42.5.0901.

(7) Gledhill, M.; van den Berg, C. M. G. Measurement of the Redox Speciation of Iron in Seawater by Catalytic Cathodic Stripping Voltammetry. *Mar. Chem.* **1995**, *50* (1–4), 51–61. https://doi.org/10.1016/0304-4203(95)00026-N.

(8) van den Berg, C. M. G. Evidence for Organic Complexation of Iron in Seawater. *Mar. Chem.* **1995**, *50* (1–4), 139–157. https://doi.org/10.1016/0304-

4203(95)00032-M.

(9) Yokoi, K.; van den Berg, C. M. G. The Determination of Iron in Seawater Using Catalytic Cathodic Stripping Voltammetry. *Electroanalysis* **1992**, *4* (1), 65–69. https://doi.org/10.1002/elan.1140040113.

(10) Kuma, K.; Nishioka, J.; Matsunaga, K. Controls on Iron(III) Hydroxide Solubility in Seawater: The Influence of PH and Natural Organic Chelators. *Limnol. Oceanogr.* **1996**, *41* (3), 396–407. https://doi.org/10.4319/lo.1996.41.3.0396.

(11) Kuma, K.; Katsumoto, A.; Kawakami, H.; Takatori, F.; Matsunaga, K. Spatial Variability of Fe(III) Hydroxide Solubility in the Water Column of the Northern North Pacific Ocean. *Deep - Sea Res. Part I - Oceanogr. Res. Pap.* **1998**, *45* (1), 91–113. https://doi.org/10.1016/S0967-0637(97)00067-8.

(12) Liu, X.; Millero, F. The Solubility of Iron in Seawater. *Mar. Chem.* **2002**, *77*, 43–54.

(13) Gledhill, M.; Buck, K. N. The Organic Complexation of Iron in the Marine Environment: A Review. *Front. Microbiol.* **2012**, *3*, 1–17. https://doi.org/10.3389/fmicb.2012.00069.

(14) Vraspir, J. M.; Butler, A. Chemistry of Marine Ligands and Siderophores. *Ann. Rev. Mar. Sci.* **2009**, *1* (1), 43–63. https://doi.org/10.1146/annurev.marine.010908.163712.

(15) Caprara, S.; Buck, K. N.; Gerringa, L. J. A.; Rijkenberg, M. J. A.; Monticelli, D. A Compilation of Iron Speciation Data for Open Oceanic Waters. *Front. Mar. Sci.* **2016**, *3* (NOV), 1–7. https://doi.org/10.3389/fmars.2016.00221.

(16) Gerringa, L. J. A.; Gledhill, M.; Ardiningsih, I.; Muntjewerf, N.; Laglera, L. M. Comparing CLE-AdCSV Applications Using SA and TAC to Determine the Fe-Binding Characteristics of Model Ligands in Seawater. *Biogeosciences* **2021**, *18* (19), 5265–5289. https://doi.org/10.5194/bg-18-5265-2021.

(17) Cullen, J. T.; Bergquist, B. A.; Moffett, J. W. Thermodynamic Characterization of the Partitioning of Iron between Soluble and Colloidal Species in the Atlantic Ocean. *Mar. Chem.* **2006**, *98* (2–4), 295–303. https://doi.org/10.1016/j.marchem.2005.10.007.

(18) Buck, K. N.; Selph, K. E.; Barbeau, K. A. Iron-Binding Ligand Production and Copper Speciation in an Incubation Experiment of Antarctic Peninsula Shelf Waters from the Bransfield Strait, Southern Ocean. *Mar. Chem.* **2010**, *122* (1–4), 148–159. https://doi.org/10.1016/j.marchem.2010.06.002.

(19) Ibisanmi, E.; Sander, S. G.; Boyd, P. W.; Bowie, A. R.; Hunter, K. A. Vertical Distributions of Iron-(III) Complexing Ligands in the Southern Ocean. *Deep Sea Res. Part II Top. Stud. Oceanogr.* **2011**, *58* (21–22), 2113–2125. https://doi.org/10.1016/j.dsr2.2011.05.028.

(20) Buck, K. N.; Sedwick, P. N.; Sohst, B.; Carlson, C. A. Organic Complexation of Iron in the Eastern Tropical South Pacific: Results from US GEOTRACES Eastern Pacific Zonal Transect (GEOTRACES Cruise GP16). *Mar. Chem.* **2018**, *201* (October 2017), 229–241. https://doi.org/10.1016/j.marchem.2017.11.007.

(21) Buck, K.; Lohan, M.; Berger, C.; Bruland, K. Dissolved Iron Speciation in Two Distinct River Plumes and an Estuary : Implications for Riverine Iron Supply.

*Limnol. Oceanogr.* **2007**, *52* (2), 843–855.

(22) Bundy, R. M.; Abdulla, H. A. N.; Hatcher, P. G.; Biller, D. V.; Buck, K. N.; Barbeau, K. A. Iron-Binding Ligands and Humic Substances in the San Francisco Bay Estuary and Estuarine-Influenced Shelf Regions of Coastal California. *Mar. Chem.* **2015**, *173*, 183–194. https://doi.org/10.1016/j.marchem.2014.11.005.

(23) Boye, M.; Aldrich, A. P.; van den Berg, C. M. .; de Jong, J. T. .; Veldhuis, M.; de Baar, H. J. . Horizontal Gradient of the Chemical Speciation of Iron in Surface Waters of the Northeast Atlantic Ocean. *Mar. Chem.* **2003**, *80* (2–3), 129–143. https://doi.org/10.1016/S0304-4203(02)00102-0.

(24) Batchelli, S.; Muller, F. L. L.; Chang, K.-C.; Lee, C. Evidence for Strong but Dynamic Iron-Humic Colloidal Associations in Humic-Rich Coastal Waters. *Environ. Sci. Technol.* **2010**, *44* (22), 8485–8490. https://doi.org/10.1021/es101081c.

(25) Laglera, L. M.; van den Berg, C. M. G. Evidence for Geochemical Control of Iron by Humic Substances in Seawater. *Limnol. Oceanogr.* **2009**, *54* (2), 610–619.

(26) Hassler, C.; Cabanes, D.; Blanco-Ameijeiras, S.; Sander, S. G.; Benner, R. Importance of Refractory Ligands and Their Photodegradation for Iron Oceanic Inventories and Cycling. *Mar. Freshw. Res.* **2020**, *71* (3), 311–320. https://doi.org/10.1071/MF19213.

(27) Norman, L.; Worms, I. A. M.; Angles, E.; Bowie, A. R.; Nichols, C. M.; Ninh Pham, A.; Slaveykova, V. I.; Townsend, A. T.; David Waite, T.; Hassler, C. S. The Role of Bacterial and Algal Exopolymeric Substances in Iron Chemistry. *Mar.*

662 *Chem.* **2015**, *173*, 148–161. https://doi.org/10.1016/j.marchem.2015.03.015.

663 (28) Hassler, C. S.; Schoemann, V.; Nichols, C. M.; Butler, E. C. V.; Boyd, P. W.
664 Saccharides Enhance Iron Bioavailability to Southern Ocean Phytoplankton. *Proc.*
665 *Natl. Acad. Sci.* **2011**, *108* (3), 1076–1081.
666 https://doi.org/10.1073/pnas.1010963108.

667 (29) Whitby, H.; Planquette, H.; Cassar, N.; Bucciarelli, E.; Osburn, C. L.; Janssen, D.
668 J.; Cullen, J. T.; González, A. G.; Völker, C.; Sarthou, G. A Call for Refining the
669 Role of Humic-like Substances in the Oceanic Iron Cycle. *Sci. Rep.* **2020**, *10* (1),
670 1–12. https://doi.org/10.1038/s41598-020-62266-7.

671 (30) Gledhill, M.; McCormack, P.; Ussher, S.; Achterberg, E. P.; Mantoura, R. F. C.;
672 Worsfold, P. J. Production of Siderophore Type Chelates by Mixed
673 Bacterioplankton Populations in Nutrient Enriched Seawater Incubations. *Mar.*
674 *Chem.* **2004**, *88* (1–2), 75–83. https://doi.org/10.1016/j.marchem.2004.03.003.

675 (31) Mawji, E.; Gledhill, M.; Milton, J. A.; Tarran, G. A.; Ussher, S.; Thompson, A.;
676 Wolff, G. A.; Worsfold, P. J.; Achterberg, E. P. Hydroxamate Siderophores:
677 Occurrence and Importance in the Atlantic Ocean. *Environ. Sci. Technol.* **2008**, *42*
678 (23), 8675–8680.

679 (32) Velasquez, I.; Nunn, B. L.; Ibisanmi, E.; Goodlett, D. R.; Hunter, K. A.; Sander, S.
680 G. Detection of Hydroxamate Siderophores in Coastal and Sub-Antarctic Waters
681 off the South Eastern Coast of New Zealand. *Mar. Chem.* **2011**, *126* (1–4), 97–
682 107. https://doi.org/10.1016/j.marchem.2011.04.003.

683 (33) Macrellis, H. M.; Trick, C. G.; Rue, E. L.; Smith, G.; Bruland, K. W. Collection

and Detection of Natural Iron-Binding Ligands from Seawater. *Mar. Chem.* **2001**, *76* (3), 175–187. https://doi.org/10.1016/S0304-4203(01)00061-5.

(34) Boiteau, R. M.; Mende, D. R.; Hawco, N. J.; McIlvin, M. R.; Fitzsimmons, J. N.; Saito, M. A.; Sedwick, P. N.; Delong, E. F.; Repeta, D. J. Siderophore-Based Microbial Adaptations to Iron Scarcity across the Eastern Pacific Ocean. *Proc. Natl. Acad. Sci.* **2016**, *113* (50), 14237–14242. https://doi.org/10.1073/pnas.1608594113.

(35) Boiteau, R. M.; Till, C. P.; Coale, T. H.; Fitzsimmons, J. N.; Bruland, K. W.; Repeta, D. J. Patterns of Iron and Siderophore Distributions across the California Current System. *Limnol. Oceanogr.* **2019**, *64* (1), 376–389. https://doi.org/10.1002/lno.11046.

(36) Bundy, R. M.; Boiteau, R. M.; McLean, C.; Turk-Kubo, K. A.; McIlvin, M. R.; Saito, M. A.; Van Mooy, B. A. S.; Repeta, D. J. Distinct Siderophores Contribute to Iron Cycling in the Mesopelagic at Station ALOHA. *Front. Mar. Sci.* **2018**, *5*. https://doi.org/10.3389/fmars.2018.00061.

(37) Hudson, R. J. .; Covault, D. T.; Morel, F. M. . Investigations of Iron Coordination and Redox Reactions in Seawater Using 59Fe Radiometry and Ion-Pair Solvent Extraction of Amphiphilic Iron Complexes. *Mar. Chem.* **1992**, *38* (3–4), 209–235. https://doi.org/10.1016/0304-4203(92)90035-9.

(38) Wu, J.; Luther, G. Complexation of Fe(III) by Natural Organic Ligands in the Northwest Atlantic Ocean by a Competitive Ligand Equilibration Method and a Kinetic Approach. *Mar. Chem.* **1995**, *50* (1–4), 159–177.

https://doi.org/10.1016/0304-4203(95)00033-N.

(39) Witter, A. E.; Hutchins, D. A.; Butler, A.; Luther, G. W. Determination of Conditional Stability Constants and Kinetic Constants for Strong Model Fe-Binding Ligands in Seawater. *Mar. Chem.* **2000**, *69*, 1–17. https://doi.org/10.1016/S0304-4203(99)00087-0.

(40) Luther, G. W.; Mullaugh, K. M.; Hauser, E. J.; Rader, K. J.; Di, D. M. Determination of Ambient Dissolved Metal Ligand Complexation Parameters via Kinetics and Pseudo-Voltammetry Experiments. *Mar. Chem.* **2021**, *234*, 103998. https://doi.org/10.1016/j.marchem.2021.103998.

(41) Witter, A. E.; Luther, G. W. Variation in Fe-Organic Complexation with Depth in the Northwestern Atlantic Ocean as Determined Using a Kinetic Approach. *Mar. Chem.* **1998**, *62* (3–4), 241–258. https://doi.org/10.1016/S0304-4203(98)00044-9.

(42) Croot, P. L.; Heller, M. I.; Schlosser, C.; Wuttig, K. Utilizing Radioisotopes for Trace Metal Speciation Measurements in Seawater. *Radioisot. - Appl. Phys. Sci.* **2011**. https://doi.org/10.5772/23182.

(43) Croot, P. L.; Heller, M. I. The Importance of Kinetics and Redox in the Biogeochemical Cycling of Iron in the Surface Ocean. *Front. Microbiol.* **2012**, *3* (June), 1–15. https://doi.org/10.3389/fmicb.2012.00219.

(44) Conway, T. M.; John, S. G. Quantification of Dissolved Iron Sources to the North Atlantic Ocean. *Nature* **2014**, *511* (7508), 212–215. https://doi.org/10.1038/nature13482.

(45) Lacan, F.; Radic, A.; Jeandel, C.; Poitrasson, F.; Sarthou, G.; Pradoux, C.;

728 Freydier, R. Measurement of the Isotopic Composition of Dissolved Iron in the
729 Open Ocean. *Geophys. Res. Lett.* **2008**, *35* (24), 1–5.
730 https://doi.org/10.1029/2008GL035841.

731 (46) Radic, A.; Lacan, F.; Murray, J. W. Iron Isotopes in the Seawater of the Equatorial
732 Pacific Ocean: New Constraints for the Oceanic Iron Cycle. *Earth Planet. Sci.*
733 *Lett.* **2011**, *306* (1–2), 1–10. https://doi.org/10.1016/j.epsl.2011.03.015.

734 (47) Ito, H.; Fujii, M.; Masago, Y.; Waite, T. D.; Omura, T. Effect of Ionic Strength on
735 Ligand Exchange Kinetics between a Mononuclear Ferric Citrate Complex and
736 Siderophore Desferrioxamine B. *Geochim. Cosmochim. Acta* **2015**, *154*, 81–97.
737 https://doi.org/10.1016/j.gca.2015.01.020.

738 (48) Ito, H.; Fujii, M.; Masago, Y.; Yoshimura, C.; Waite, T. D.; Omura, T. Mechanism
739 and Kinetics of Ligand Exchange between Ferric Citrate and Desferrioxamine B.
740 *J. Phys. Chem. A* **2011**, *115* (21), 5371–5379. https://doi.org/10.1021/jp202440e.

741 (49) Boiteau, R. M.; Fitzsimmons, J. N.; Repeta, D. J.; Boyle, E. A. Detection of Iron
742 Ligands in Seawater and Marine Cyanobacteria Cultures by High-Performance
743 Liquid Chromatography–Inductively Coupled Plasma-Mass Spectrometry. *Anal.*
744 *Chem.* **2013**, *85* (9), 4357–4362. https://doi.org/10.1021/ac3034568.

745 (50) Heumann, K. G.; Gallus, S. M.; Ra, G.; Vogl, J. Precision and Accuracy in Isotope
746 Ratio Measurements by Plasma Source Mass Spectrometry †. *J. Anal. At.*
747 *Spectrom.* **1998**, *13* (September).

748 (51) Gerringa, L. J. A.; Rijkenberg, M. J. A.; Wolterbeek, H. T.; Verburg, T. G.; Boye,
749 M.; de Baar, H. J. W. Kinetic Study Reveals Weak Fe-Binding Ligand, Which

Affects the Solubility of Fe in the Scheldt Estuary. *Mar. Chem.* **2007**, *103* (1–2), 30–45. https://doi.org/10.1016/j.marchem.2006.06.002.

(52) Luther, G. W.; Wu, J. What Controls Dissolved Iron Concentrations in the World Ocean? — A Comment. *Mar. Chem.* **1997**, *57* (3–4), 173–179. https://doi.org/10.1016/S0304-4203(97)00046-7.

(53) Silva, A. M. N.; Kong, X.; Parkin, M. C.; Cammack, R.; Hider, R. C. Iron(Iii) Citrate Speciation in Aqueous Solution. *Dalt. Trans.* **2009**, No. 40, 8616–8625. https://doi.org/10.1039/b910970f.

(54) Morel, F. M.; Hering, J. *Principles And Applications Of Aquatic Chemistry.*, 2nd ed.; Wiley: New York, NY, 1993.

(55) Anderegg, G.; L'Eplattenier, F.; Schwarzenbach, G. Hydroxamatkomplexe III. Eisen(III)-Austausch Zwischen Sideraminen Und Komplexonen. Diskussion Der Bildungskonstanten Der Hydroxamatkomplexe. *Helv. Chim. Acta* **1963**, *46* (4), 1409–1422. https://doi.org/10.1002/hlca.19630460436.

(56) Anderegg, G.; L'Eplattenier, F.; Schwarzenbach, G. Hydroxamatkomplexe II. Die Anwendung Der PH-Methode. *Helv. Chim. Acta* **1963**, *46* (4), 1400–1408. https://doi.org/10.1002/hlca.19630460435.

(57) Schlosser, C.; Croot, P. L. Application of Cross-Flow Filtration for Determining the Solubility of Iron Species in Open Ocean Seawater. *Limnol. Oceanogr. Methods* **2008**, *6*, 630–642. https://doi.org/10.4319/lom.2008.6.630.

(58) Rijkenberg, M. J. A.; Gerringa, L. J. A.; Carolus, V. E.; Velzeboer, I.; de Baar, H. J. W. Enhancement and Inhibition of Iron Photoreduction by Individual Ligands in

Open Ocean Seawater. *Geochim. Cosmochim. Acta* **2006**, *70* (11), 2790–2805. https://doi.org/10.1016/j.gca.2006.03.004.

(59) Tufano, T. P.; Raymond, K. N. Coordination Chemistry of Microbial Iron Transport Compounds. 21. Kinetics and Mechanism of Iron Exchange in Hydroxamate Siderophore Complexes. *J. Am. Chem. Soc.* **1981**, *103* (22), 6617–6624. https://doi.org/10.1021/ja00412a015.

(60) Raymond, K. N.; Mueller, G.; Matzanke, B.; Müller, G. Complexation of Iron by Siderophores a Review of Their Solution and Structural Chemistry and Biological Function. *Struct. Chem.* **1984**, *123*, 49–102. https://doi.org/10.1021/ba-1977-0162.ch002.

(61) Rea, L. T.; Xu, Y.; Boland, N. E. Effects of Calcium on the Kinetics of a Model Disjunctive Ligand Exchange Reaction: Implications for Dynamic Trace Metal Ion Speciation. *Environ. Sci. Process. Impacts* **2019**, *21* (1), 89–103. https://doi.org/10.1039/c8em00301g.

(62) Hayes, C. T.; Fitzsimmons, J. N.; Boyle, E. A.; McGee, D.; Anderson, R. F.; Weisend, R.; Morton, P. L. Thorium Isotopes Tracing the Iron Cycle at the Hawaii Ocean Time-Series Station ALOHA. *Geochim. Cosmochim. Acta* **2015**, *169*, 1–16. https://doi.org/10.1016/j.gca.2015.07.019.

(63) Croot, P. L. Short Residence Time for Iron in Surface Seawater Impacted by Atmospheric Dry Deposition from Saharan Dust Events. *Geophys. Res. Lett.* **2004**, *31* (23), L23S08. https://doi.org/10.1029/2004GL020153.

(64) Hering, J. G.; Morel, F. M. M. Slow Coordination Reactions in Seawater.

794 *Geochim. Cosmochim. Acta* **1989**, *53* (3), 611–618. https://doi.org/10.1016/0016-
795 7037(89)90004-5.

796 (65) Bundy, R. M.; Biller, D. V; Buck, K. N.; Bruland, K. W.; Barbeau, K. A. Distinct
797 Pools of Dissolved Iron-Binding Ligands in the Surface and Benthic Boundary
798 Layer of the California Current. *Limnol. Oceanogr.* **2014**, *59* (3), 769–787.
799 https://doi.org/10.4319/lo.2014.59.3.0769.

800 (66) Hering, J.; Morel, F. Kinetics of Trace Metal Complexation: Ligand-Exchange
801 Reactions. *Environ. Sci. Technol.* **1990**, *252* (9), 242–252. https://doi.org/0013-
802 936X/90/0924-0242.

803